MULTIDI SCIENCE
Journal of Multidisciplinary Science
Vol. 3 No. 2, June 2026, Pages. 151-167
P-ISSN: 3046-692X, E-ISSN: 3046-6911
Doi: 10.59631/multidiscience.v3i2.513

Evaluation of the Influence of Measurement Noise and Adaptive Gain Adjustment in Kalman Filtering for Estimating Angular Coordinates of Randomly Maneuvering Targets

Vu Quang Luong[1*], Trinh Thi Minh[1]
[1]Air Defence-Air Force Academy, Viet Nam

** Corresponding Email: vuquangluong88@gmail.com*

Abstract
Accurate state estimation in nonlinear dynamic systems is a fundamental requirement in many engineering applications, particularly when system noise characteristics vary over time. Conventional Kalman filters (KF) often suffer from performance degradation under time-varying noise conditions due to their reliance on fixed noise covariance assumptions. The objective of this paper is to present a comprehensive performance analysis of conventional KF and adaptive KF (AKF) for nonlinear state estimation in a fourth-order dynamic system. Methodologically, the study employs a comparative quantitative simulation design, focusing on evaluating estimation accuracy, convergence behavior, and statistical consistency under different process and measurement noise conditions. The proposed framework incorporates an adaptive mechanism for updating noise covariance matrices based on innovation statistics. Simulation results demonstrate that the adaptive KF significantly improves estimation accuracy and stability compared to the conventional KF, particularly in scenarios with rapidly changing noise characteristics. These findings confirm the effectiveness of adaptive filtering strategies and highlight their potential for practical applications in control and navigation systems.

Keywords: Adaptive kalman filter, kalman filter, nonlinear systems, state estimation, time-varying noise.

1. Introduction

Accurate state estimation is a fundamental requirement in many engineering systems (Mursyitah et al., 2025; Sheikh, 2023), especially in control, navigation, and target-tracking applications where system states cannot be measured directly and must be reconstructed from noisy observations. For such problems, Kalman-based estimation remains one of the most widely used frameworks because of its recursive structure and strong theoretical foundation. However, when the underlying dynamics are nonlinear, the estimation performance depends strongly on model fidelity, linearization quality, and the correctness of noise assumptions. As nonlinearities become stronger, conventional filtering methods may experience increased bias, slower convergence, and degraded robustness (Chen et al., 2025; Ding & Wen, 2024; Peng et al., 2023).

To handle nonlinear systems, various extensions of the classical Kalman filter have been proposed (Anagnostaki et al., 2026), including the extended Kalman filter (Habib et al., 2025) and high-order Kalman filtering formulations (Ding & Wen, 2024). These methods attempt to improve estimation accuracy by using first-order or higher-order approximations of the nonlinear state and measurement equations. Recent studies have shown that high-order filtering can provide better estimation performance than conventional first-order linearization, particularly in systems with complex nonlinear structures and high-order state variables (Ding & Wen, 2024; Peng et al., 2023). Nevertheless, these approaches are still sensitive to modeling mismatch and may lose effectiveness when the system is affected by uncertain or time-varying noise.

In parallel with the development of high-order filtering, recent research has also explored data-driven and learning-based enhancements to Kalman filtering. Neural-assisted filtering methods have attracted considerable attention because they can compensate for unknown nonlinear dynamics while preserving part of the interpretability of model-based filters. Examples include deterministic learning-based EKF models and neural network aided Kalman filtering architectures, which have demonstrated improved performance for nonlinear dynamical systems and partially known models (Alanis, 2025; Eang & Lee, 2024; Stubberud & Kramer, 2023; Wang & Shen, 2024; Wu et al., 2025). These results confirm that Kalman filtering can be significantly strengthened when adaptive or learning mechanisms are incorporated into the estimation process.

Despite these advances, an important limitation remains. Many existing studies focus on proposing new filter structures or improving approximation accuracy, but fewer works provide a systematic analysis of how noise variation affects filter behavior, especially in terms of gain adaptation, estimation stability, and tracking accuracy across different operating conditions. In practical systems, measurement noise is often nonstationary and may change over time because of environmental variation, sensor quality, operating range, or target maneuvering conditions. Under such circumstances, the use of fixed-noise assumptions in conventional Kalman filtering can lead to suboptimal gain selection and reduced estimation quality, while adaptive filtering strategies may offer better robustness (Ge et al., 2019; Kruse et al., 2025). However, comparative assessments between fixed and adaptive Kalman filtering under controlled time-varying noise scenarios are still relatively limited in the recent literature.

Driven by this research gap, the urgency to quantitatively evaluate how noise variations impact gain adaptation has become increasingly critical. Therefore, the primary objective of this study is to conduct an in-depth performance analysis between conventional and adaptive Kalman filtering for estimating the angular coordinates of randomly maneuvering targets under time-varying noise conditions. This paper contributes a comprehensive evaluation framework that elucidates the practical benefits of adaptive noise covariance updating mechanisms. The benefits of this study go beyond providing a deeper understanding of filter behavior in uncertain environments; they also offer a crucial baseline for designing highly reliable target-tracking and navigation systems in real-world engineering applications.

2. Method

2.1 Research Design

This study employs a quantitative comparative simulation approach to evaluate the performance of the two filters. Synthetic data representing the kinematics of a randomly maneuvering target were generated using mathematical models implemented in MATLAB. The data collection process involved extracting the estimated Line of Sight (LOS) angle and angular velocity under three deliberately introduced levels of measurement noise. Data analysis was conducted by calculating and comparing the Root Mean Square Error (RMSE) between the estimated values and the true states, thereby providing an objective metric of the accuracy and stability of the adaptive gain updating mechanism.

2.2. Nonlinear System Model

Consider the motion of a target in a plane, with the observed variable being the LOS angle ϕ_k. The system state is described by the vector:

$$\boldsymbol{x}_k = \begin{bmatrix} \phi_k \\ \omega_k \\ \dot{\omega}_k \end{bmatrix} \tag{1}$$

Where:

ϕ_k : LOS angle (deg);

ω_k : angular velocity (deg/s);

$\dot{\omega}_k$: angular acceleration (deg/s^2).

The discrete model with sampling period T is given by:

$$\boldsymbol{x}_{k+1} = \boldsymbol{F}\boldsymbol{x}_k + \mathbf{w}_k \tag{2}$$

with the state transition matrix:

$$F = \begin{bmatrix} 1 & T & \frac{T^2}{2} \\ 0 & 1 & T \\ 0 & 0 & 1 \end{bmatrix} \quad (3)$$

and the process noise $\mathbf{w}_k \sim N(0, \boldsymbol{Q}_k)$.

The measurement equation is described by:

$$z_k = \boldsymbol{H}\boldsymbol{x}_k + v_k, \ \boldsymbol{H} = \begin{bmatrix} 1 & 0 & 0 \end{bmatrix} \quad (4)$$

where $v_k \sim N(0, R_k)$ is the random measurement noise.

2.3. Noise Model and Parameter σ

The process noise simulating random maneuvering acceleration has a standard deviation of σ_a. The power spectral density of the process noise is defined as:

$$q_a = \sigma_a^2 \quad (5)$$

The process noise covariance matrix $\boldsymbol{Q}_k$ is determined according to (2):

$$\boldsymbol{Q}_k = q_a \begin{bmatrix} \frac{T^5}{20} & \frac{T^4}{8} & \frac{T^3}{6} \\ \frac{T^4}{8} & \frac{T^3}{3} & \frac{T^2}{2} \\ \frac{T^3}{6} & \frac{T^2}{2} & T \end{bmatrix} \quad (6)$$

The measurement noise is assumed to have variance $R_k = \sigma_v^2$. When the noise varies with time:

$$R_k = R_0 \left[1 + \delta_R \sin(2\pi f_R kT)\right] + \eta_R(k) \quad (7)$$

Where:

$R_0 = \sigma_{v0}^2$: average variance;

δ_R : relative oscillation amplitude (0–1);

f_R : slow fluctuation frequency;

$\eta_R(k)$: small white noise (to increase randomness).

During simulation, the measurement noise is generated by:

$$v_k \sim N(0, \sigma_v^2(k)), \sigma_v = \sqrt{\sigma_{v0}^2 \left[1 + \delta_R \sin(2\pi f_R kT)\right] + \eta_R(k)} \quad (8)$$

2.4. Kalman Filter

Stage 1: Prediction

$$\widehat{\boldsymbol{x}}_{k|k-1} = \boldsymbol{F}\widehat{\boldsymbol{x}}_{k-1|k-1} \tag{9}$$

$$\boldsymbol{P}_{k|k-1} = \boldsymbol{F}\boldsymbol{P}_{k-1|k-1}\boldsymbol{F}^T + \boldsymbol{Q}_k \tag{10}$$

Stage 2: Update

Innovation:

$$\tilde{y}_k = z_k - \boldsymbol{H}\widehat{\boldsymbol{x}}_{k|k-1} \tag{11}$$

Innovation covariance:

$$S_k = \boldsymbol{H}\boldsymbol{P}_{k|k-1}\boldsymbol{H}^T + R_k \tag{12}$$

Kalman gain:

$$\boldsymbol{K}_k = \boldsymbol{P}_{k|k-1}\boldsymbol{H}^T S_k^{-1} \tag{13}$$

Updated estimate:

$$\widehat{\boldsymbol{x}}_{k|k} = \widehat{\boldsymbol{x}}_{k|k-1} + \boldsymbol{K}_k\tilde{y}_k \tag{14}$$

Updated covariance:

$$\boldsymbol{P}_{k|k} = (I - \boldsymbol{K}_k\boldsymbol{H})\boldsymbol{P}_{k|k-1} \tag{15}$$

Scalar form of the Kalman gain:

$$K_k = \frac{P_{\phi\phi,k|k-1}}{P_{\phi\phi,k|k-1} + R_k} = \frac{P_{\phi\phi,k|k-1}}{P_{\phi\phi,k|k-1} + \sigma_v^2} = \frac{P_{\phi\phi,k|k-1}}{P_{\phi\phi,k|k-1} + \sigma_{v0}^2\left[1 + \delta_R \sin(2\pi f_R kT)\right] + \eta_R(k)} \tag{16}$$

Derivative of K_k with respect to measurement noise σ:

$$\frac{\partial K_k}{\partial \sigma_v} = -\frac{2\sigma_v P_{\phi\phi,k|k-1}}{(P_{\phi\phi,k|k-1} + \sigma_v^2)^2} = -\frac{2\sigma_v P_{\phi\phi,k|k-1}}{(P_{\phi\phi,k|k-1} + \sigma_{v0}^2\left[1 + \delta_R \sin(2\pi f_R kT)\right] + \eta_R(k))^2} < 0 \tag{17}$$

When σ increases, K_k decreases (smoother filtering, slower response); σ when σ decreases, K_k increases (faster but noisier filtering).

2.5. Adaptive Kalman Filter

To handle cases where the measurement noise changes or is unknown, R_k and Q_k are updated adaptively according to the residual energy and estimation error.

Adaptive update of measurement noise:

$$\widehat{R}_k = \lambda \widehat{R}_{k-1} + (1-\lambda)\left[\tilde{y}_k^2 - \boldsymbol{H}\boldsymbol{P}_{k|k-1}\boldsymbol{H}^T \right] \tag{18}$$

Where $0 < \lambda < 1$ is the forgetting factor.

$$\widehat{\sigma}_v(k) = \sqrt{\widehat{R}_k} \tag{19}$$

Adaptive update of process noise:

$$\widehat{Q}_k = \beta \widehat{Q}_{k-1} + (1-\beta)\left[\boldsymbol{K}_k \tilde{y}_k \tilde{y}_k^T - (\boldsymbol{P}_{k|k-1} - \boldsymbol{P}_{k|k}) \right] \tag{20}$$

Where $0 < \beta < 1$ is the smoothing factor. After obtaining $\widehat{R}_k$ and $\widehat{Q}_k$, the Kalman gain is recalculated:

$$\boldsymbol{K}_k = \boldsymbol{P}_{k|k-1}\boldsymbol{H}^T (\boldsymbol{H}\boldsymbol{P}_{k|k-1}\boldsymbol{H}^T + \widehat{R}_k)^{-1} \tag{21}$$

Combining (5)–(7) and (16), the influence of noise and gain can be expressed as:

$$K_k \approx f(\sigma_a, \sigma_v) = \frac{c_1 T^2 \sigma_a^2}{c_1 T^2 \sigma_a^2 + 4\sigma_v^2} \tag{22}$$

Where c_1 is a scaling coefficient (commonly $c_1 \in [0.5, 1]$). Equation (22) clearly expresses the influence of process noise σ_a and measurement noise σ_v . When σ_a increases, increases (faster filter response, better tracking of maneuvers); when σ_v increases, K_k decreases (more stable filtering but greater phase lag).

Filter performance is evaluated based on estimation error and statistical reliability of the filtering process.

Root Mean Square Error (RMSE):

$$RMSE_\phi = \sqrt{\frac{1}{N}\sum_{k=1}^{N}\left(\widehat{\phi} - \phi_k^{true}\right)^2} \tag{23}$$

$$RMSE_\omega = \sqrt{\frac{1}{N}\sum_{k=1}^{N}\left(\widehat{\omega} - \omega_k^{true}\right)^2} \tag{24}$$

3. Results and Discussion

3.1. Simulation Setup

To verify the effectiveness of the developed KF and AKF algorithms, simulations were carried out on a randomly maneuvering target trajectory under different levels of measurement noise. The initial parameters, noise characteristics, and gain factors were varied in a controlled manner to evaluate their influence on the estimation errors of the target's LOS angle and angular velocity. The results are represented through corresponding plots and RMSE indicators.

The selected simulation parameters are as follows:

- Simulation time: 20(s);

- Sampling step: T = 0.005 (s);

- Measurement noise variance for three noise levels:

$\sigma_1^2 = 0.03(\deg^2)$, $\sigma_2^2 = 0.16(\deg^2)$, $\sigma_3^2 = 0.36(\deg^2)$;

- Initial process noise variance: $q_a = 0.01(\deg^2 / s^3)$;

- Kalman gain coefficients: $k_1 = 0.08$, $k_2 = 0.18$, $k_3 = 0.44$;

- Forgetting factor (adaptive): $\lambda = 0.1$;

- Smoothing factor: $\beta = 0.05$;

- Process noise matrix:

$$\boldsymbol{Q}_3 = q_a.Q_{base,3} = \begin{bmatrix} 1.5625\times10^{-5} & 7.8125\times10^{-3} & 2.0833\times10^{-2} \\ 7.8125\times10^{-3} & 4.1667\times10^{-2} & 1.25\times10^{-1} \\ 2.0833\times10^{-2} & 1.25\times10^{-1} & 5\times10^{-2} \end{bmatrix}$$

- Background oscillation frequency: $f_R = 0.2(Hz)$;

- Relative oscillation amplitude: $\delta_R = 0.2(\deg / s^2)$;

- Command noise amplitude (small white noise for increased randomness): $\eta_R(k) = 0.1(\deg/ s^2)$.

3.2. Estimation Performance under Time-Varying Noise

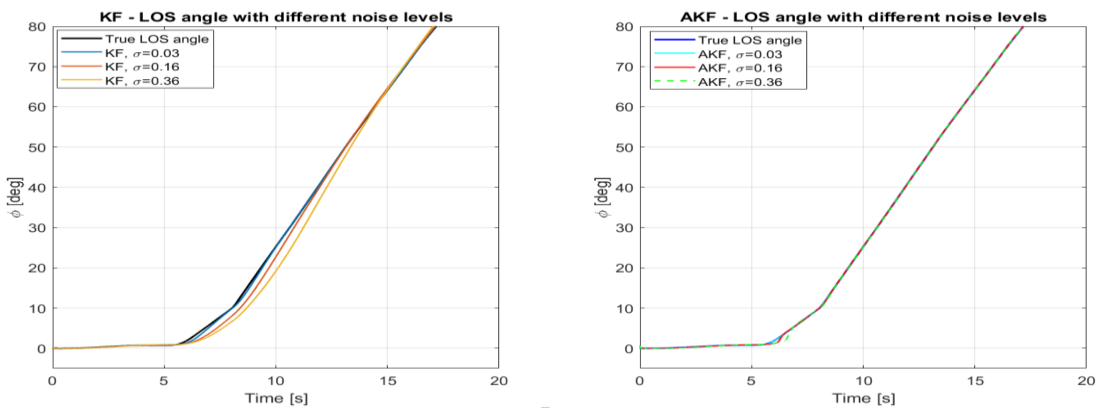

Figure 1. Comparison of Target LOS Angle at Different Noise Levels

Figure 1 shows the LOS angle tracking capability of the KF and AKF over 20 seconds under varying measurement noise levels. For the KF, the estimation quality deteriorates rapidly as σ increases. At $\sigma = 0.16$, the estimated trajectory begins to exhibit a clear lag, and at $\sigma = 0.36$, the deviation increases sharply during the maneuvering phase (8–14 s), with the peak offset of about 5–6 (deg). In contrast, the AKF maintains stable tracking across all three noise levels; the maximum deviation observed is only about 1–1.5 (deg) even at $\sigma = 0.36$. Overall, the AKF maintains smoothness and tracking accuracy almost independent of σ, whereas the KF is strongly affected as measurement noise increases.

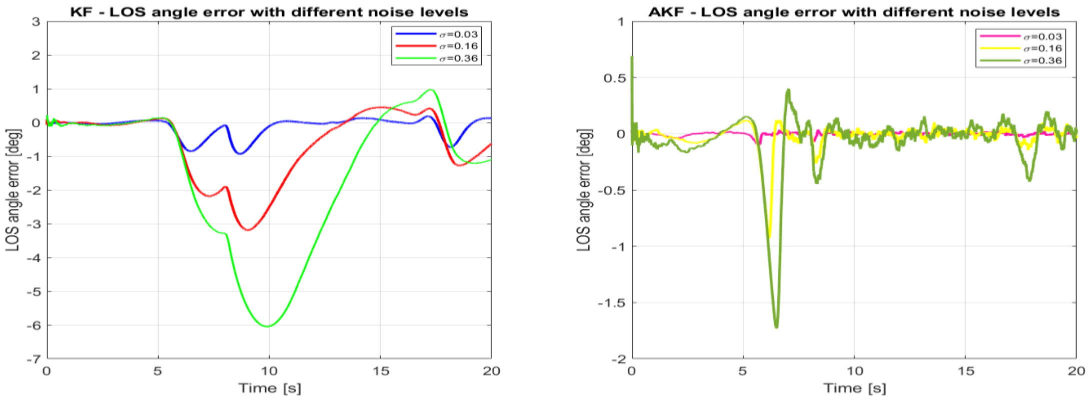

Figure 2. LOS Angle Estimation Error under Different Noise Levels

Figure 2 illustrates the estimation error, allowing clearer observation of the stability of each filter. For the KF, the error tends to become strongly negative when the target starts maneuvering: at $\sigma = 0.16$, the error reaches about −3 (deg), and at $\sigma = 0.36$ can drop to −6 (deg) before gradually returning to zero. The oscillation amplitude of the error also increases with σ, indicating the high sensitivity of KF to measurement noise. Conversely, the AKF error remains mostly within ±0.5 (deg) for $\sigma = 0.03$ and $\sigma = 0.16$, and only reaches about −1.5 (deg) at its maximum peak for $\sigma = 0.36$. After the maneuvering phase, the AKF error returns to the near-zero region faster and with smaller oscillations than KF, demonstrating that the adaptive update mechanism effectively suppresses error amplification as noise intensity and rate of change increase.

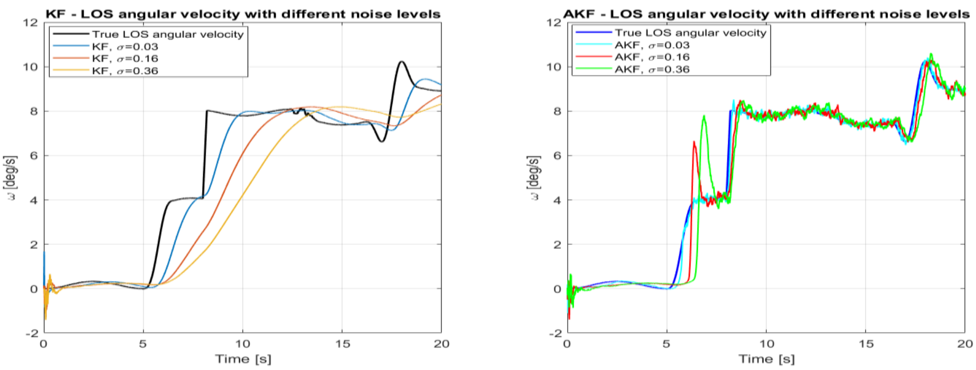

Figure 3. Comparison of Target LOS Angular Velocity under Different Noise Levels

Figure 3 shows the LOS angular velocity estimation response over 20 seconds. With the KF, as σ increases, the estimated curves lag noticeably behind the true values, especially during the acceleration phase (approximately 6–10 s). The peak deviation can reach 2–3 (deg/s) at $\sigma = 0.16$ and around 4 (deg/s) at $\sigma = 0.36$. The oscillation amplitude after the maneuvering phase also increases with σ, showing that KF becomes less stable under high measurement noise. In contrast, the AKF maintains very close tracking to the true signal for all three noise levels; the amplitude and shape of the signal remain almost unchanged as σ increases. The maximum deviation of AKF is only about 0.8–1.0 (deg/s), nearly overlapping the true angular velocity both in maneuvering and steady phases. This clearly demonstrates the effectiveness of the adaptive mechanism in adjusting noise matrices, resulting in much greater stability of AKF compared to KF.

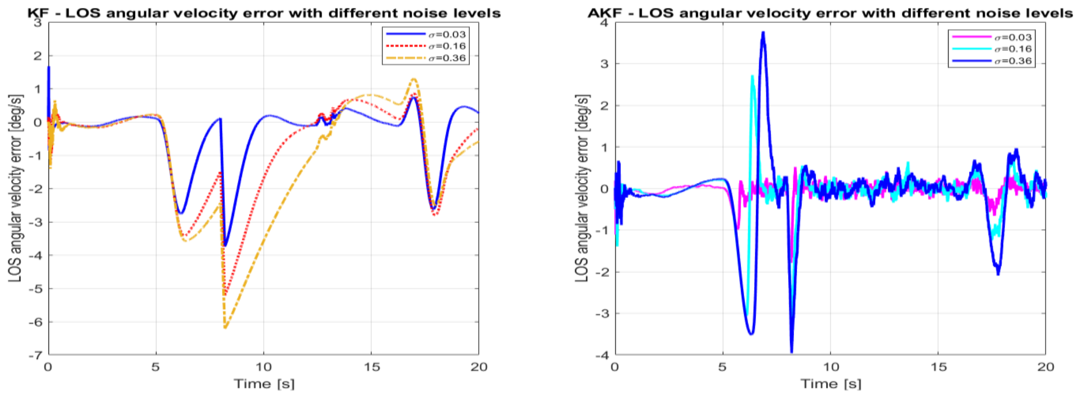

Figure 4. LOS Angular Velocity Error under Different Noise Levels

Figure 4 shows the error characteristics of the KF and AKF. For the KF, the error increases rapidly with noise level: at $\sigma = 0.03$, it oscillates within ±2 (deg/s); at $\sigma = 0.16$, it reaches −4 (deg/s); and at $\sigma = 0.36$, it can exceed −6 deg/s during strong maneuvering (~8–10 s). Afterward, the error gradually decreases but still maintains significant offset. In contrast, the AKF error is much smaller and more stable, mainly within ±1.5 (deg/s) for σ in (0.03–0.16) and ±3 (deg/s) at $\sigma = 0.36$. AKF also recovers to near-zero faster after maneuvering, without noticeable lag or residual oscillation. Together, Figures 3 and 4 show that AKF maintains an average error about 2–4 times smaller than KF and reduces peak deviation by over 50%, confirming its robustness and effective self-adjustment capability under varying noise.

3.3. Influence of Kalman Gain on Estimation Behavior

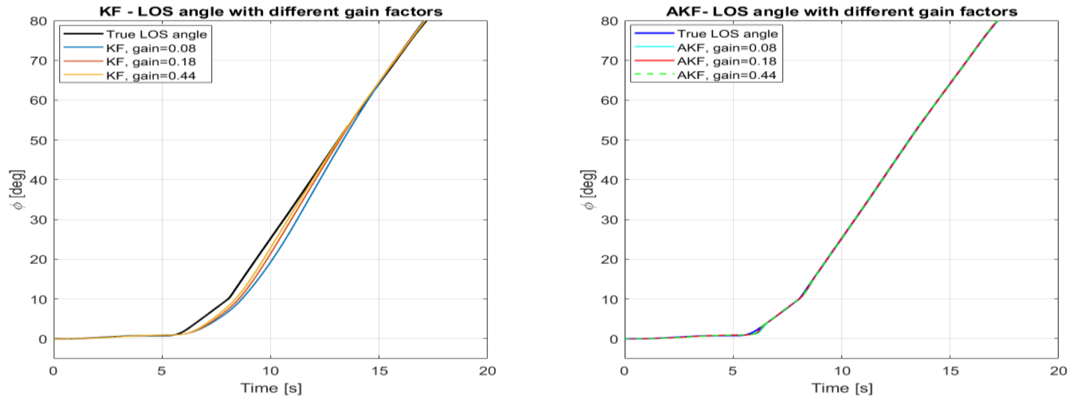

Figure 5. Comparison of Target LOS Angle under Different Gain Factors

Figure 5 shows the variation of LOS angle over time when changing the gain factor $K = 0.08, 0.18, 0.44$ for both KF and AKF. For KF, when the gain is small $(K = 0.08)$, the estimated response exhibits a significant lag compared to the true value, while larger gains ($K = 0.18$ and $K = 0.44$) allow faster response and closer tracking. However, when K becomes too large, the signal becomes more sensitive to noise, shown by small oscillations around the true value. In contrast, for AKF, the difference between the gain values is almost negligible. The adaptive filter automatically adjusts the noise matrices and gain factor over time, resulting in estimated curves nearly coinciding with the true value, proving the stability and flexibility of AKF when noise characteristics change.

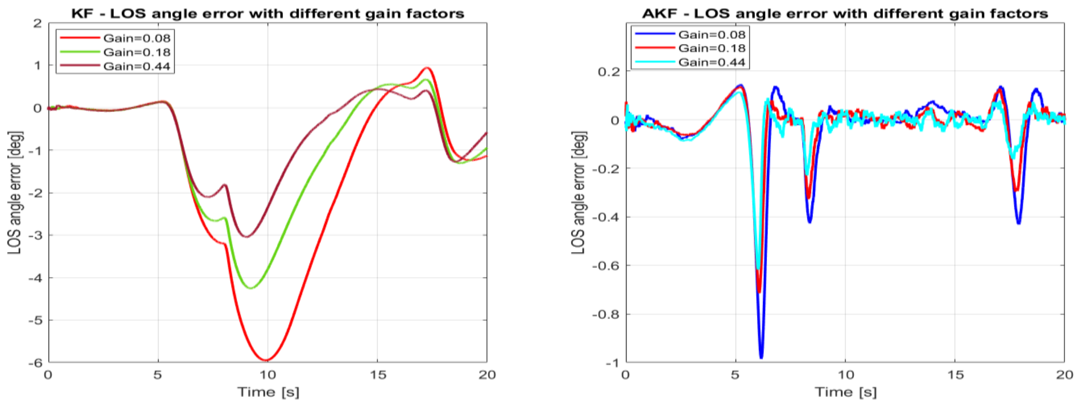

Figure 6. LOS Angle Estimation Error under Different Gain Factors

Figure 6 shows the LOS angle estimation error corresponding to different gain values. For KF, the error increases significantly when K is small (0.08), with a maximum deviation of about −6 (deg) during the maneuvering phase (8–12 s). As K increases to 0.18 and 0.44, the error gradually decreases but still exhibits clear oscillations, indicating that KF is still strongly affected by noise and not fully stable. Meanwhile, the AKF error is much smaller, with oscillation amplitude mostly within

±0.5 (deg). The error curves for different K values almost overlap, reflecting the self-adaptive capability that maintains the gain at an optimal level. Therefore, AKF achieves a mean error 4–6 times lower than KF and stabilizes quickly after maneuvering, demonstrating its superior performance under varying noise and gain conditions.

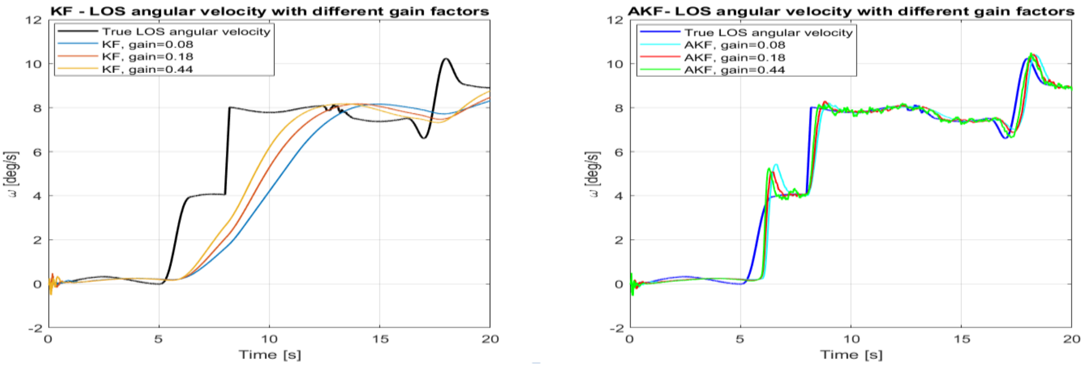

Figure 7. Comparison of Target LOS Angular Velocity under Different Gain Factors

Figure 7 illustrates the LOS angular velocity response over time for different gain factors for $K = 0.08, 0.18, 0.44$ both KF and AKF. For KF, when the gain is small $(K = 0.08)$, the estimated signal shows a noticeable lag compared to the true value, particularly during the acceleration phase (6–10 s) and the deceleration phase (15–18 s). As the gain increases to $K = 0.18$ and $K = 0.44$, the filter responds faster and follows the true curve more closely; however, during strong motion phases, oscillations and clear phase delays still occur. In contrast, with AKF, the estimated curves almost coincide with the true angular velocity at all three gain levels. Thanks to the adaptive update mechanism of the noise matrices, AKF automatically corrects the gain factor in real time, keeping the estimated signal closely aligned with the true value and eliminating most of the lag phenomenon. This shows that AKF maintains high accuracy and stability, being largely insensitive to the initial gain value.

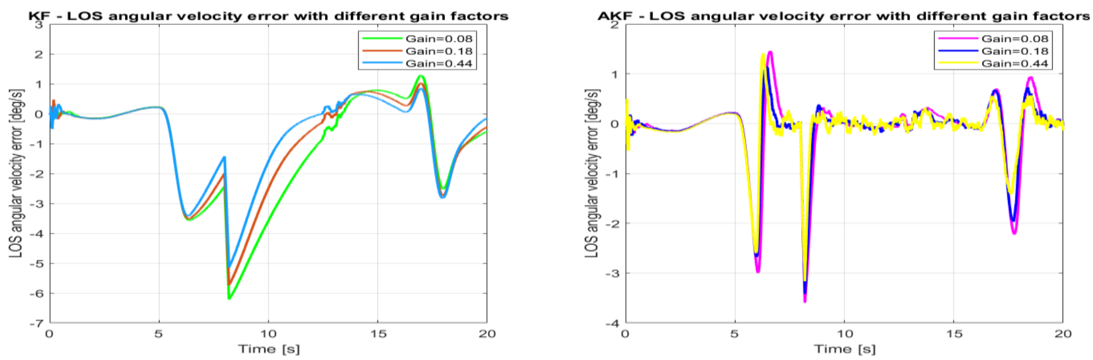

Figure 8. LOS Angular Velocity Estimation Error under Different Gain Factors

Figure 8 shows the LOS angular velocity estimation error corresponding to different gain values. For KF, the error amplitude is large and highly sensitive to changes in K : at $K = 0.08$, the maximum error can exceed −6 (deg/s) during the maneuvering phase; as K increases to 0.18 and 0.44, the error decreases but still maintains oscillations of about ±(3–4) (deg/s). This reflects the poor stability of KF when the gain is not properly adjusted to the noise characteristics. In contrast, the AKF error is much smaller and more stable, mostly within ±1 (deg/s). The error curves for different K almost coincide, demonstrating the self-adjusting capability that allows AKF to maintain optimal performance throughout the process. After maneuvering phases, the error quickly returns to near zero without noticeable residual oscillations. Taken together, these results show that AKF achieves 3–5 times higher accuracy than KF and maintains better stability across the entire gain range.

3.4. Quantitative Performance Evaluation Using RMSE

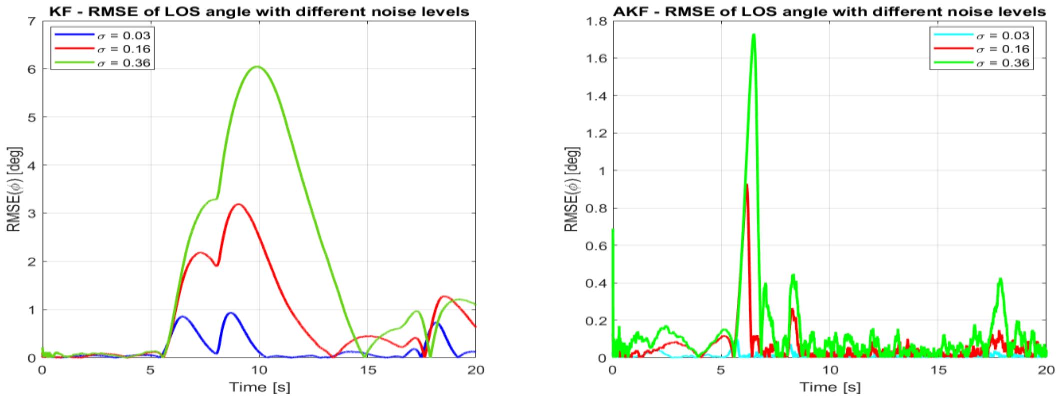

Figure 9. Comparison of Target LOS Angle RMSE under Different Noise Levels

The figure shows the RMSE of the LOS angle when using the standard KF and the AKF under different noise levels. It can be observed that for KF, when the noise standard deviation σ increases from 0.03 to 0.36, the RMSE rises sharply, reaching a maximum of about 6 degrees at the highest noise level. In contrast, AKF maintains much smaller and more stable errors, with a maximum RMSE of only about 1.7 (deg) even under strong noise. This result demonstrates that AKF has better adaptability and noise correction capability, reducing the average error by 4–6 times compared to KF under high-noise conditions.

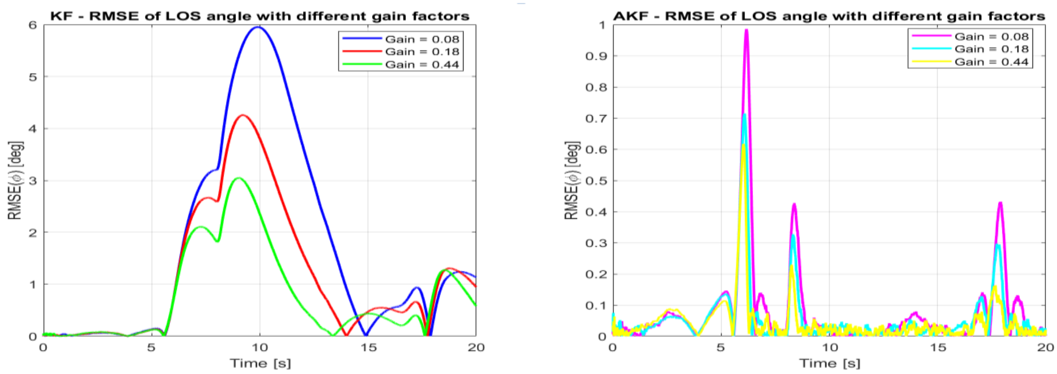

Figure 10. Comparison of Target LOS Angle RMSE under Different Gain Factors

Figure 10 illustrates the influence of the gain factor on the LOS angle RMSE when applying KF and AKF. For KF, as the gain increases from 0.08 to 0.44, the RMSE decreases significantly from approximately 6 (deg) to about 3 (deg), indicating that this filter is quite sensitive to the gain parameter. Meanwhile, AKF maintains consistently low RMSE values between 0.5 and 1 (deg), showing little sensitivity to gain variation. This confirms that AKF can automatically adjust the gain factor to match real measurement conditions, ensuring higher accuracy and stability than KF.

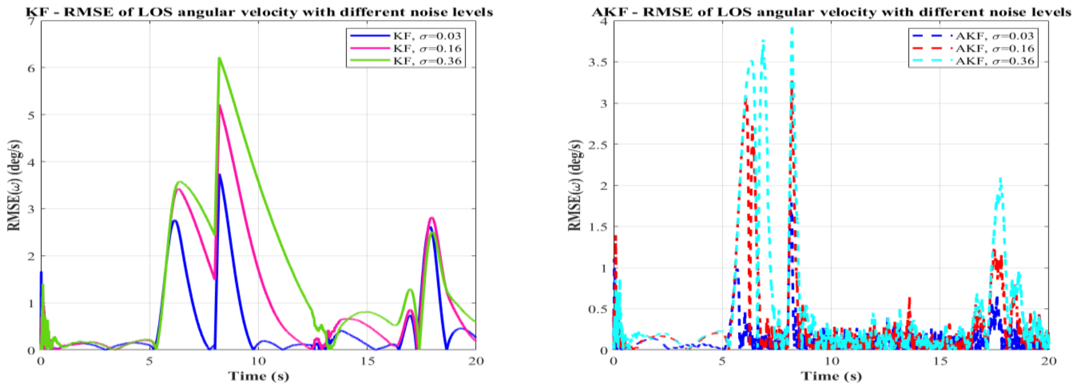

Figure 11. Comparison of LOS Angular Velocity RMSE under Different Noise Levels

The two plots illustrate how RMSE changes over time for three noise levels $(\sigma = 0.03, 0.16, 0.36)$. In the left plot (KF), the RMSE increases significantly with higher noise, especially around 7–10 (s) and 17–18 (s), showing that the standard Kalman Filter is highly sensitive to measurement noise. In contrast, the right plot shows that the AKF maintains low and stable RMSE values even when the noise increases. Although local error peaks still appear, their amplitude is significantly smaller than that of KF. This demonstrates that AKF performs more effectively in time-varying noise environments, improving the accuracy of LOS angular velocity estimation.

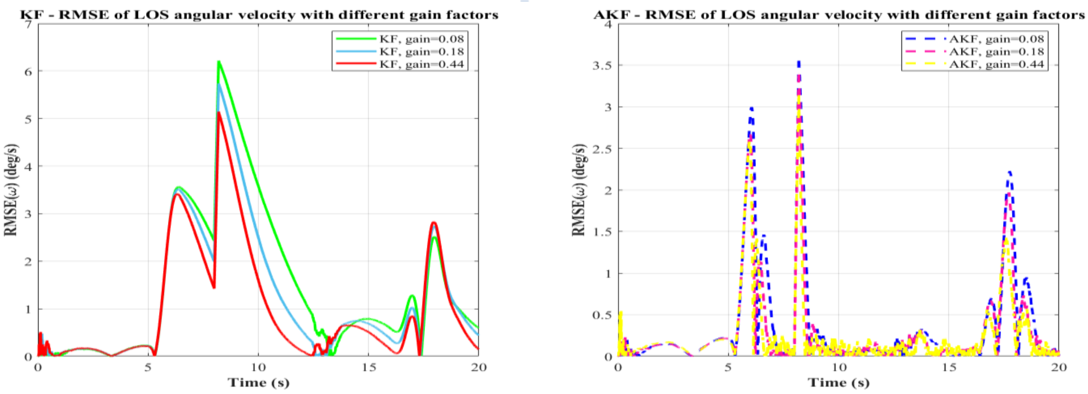

Figure 12. Comparison of LOS Angular Velocity RMSE under Different Gain Factors

The figure clearly shows the difference in filtering efficiency between the two methods. For the standard KF, the maximum RMSE of LOS angular velocity reaches about 6.3 (deg/s) around 9 (s), with an average value of about 1.5–2.0 (deg/s) across the time domain. As the gain increases from 0.08 to 0.44, the RMSE amplitude decreases slightly but still exhibits large error peaks. In contrast, with the AKF, the maximum RMSE drops to about 3.5 (deg/s), corresponding to a nearly 45% reduction compared to KF, while the average error decreases to below 1 deg/s. Thus, AKF not only significantly reduces instantaneous errors but also maintains higher overall stability throughout the simulation, proving its ability to adapt effectively to time-varying measurement noise.

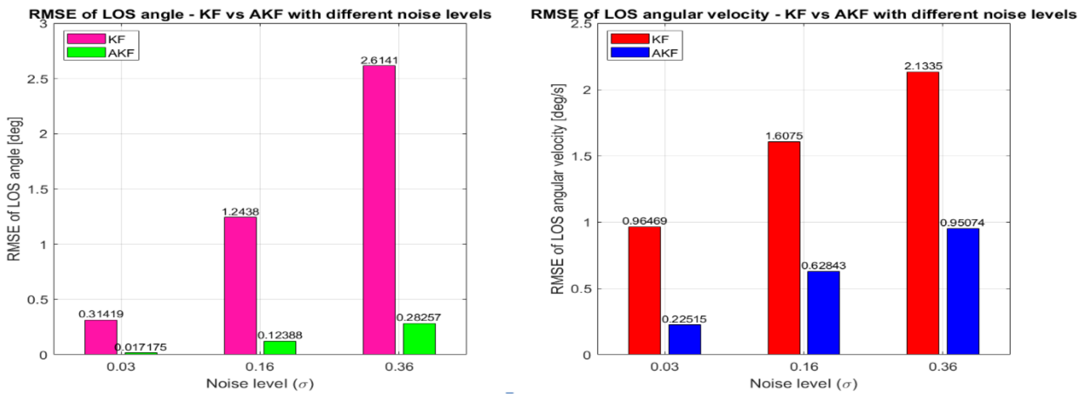

Figure 13. Comparison of Average RMSE of LOS Angle and Angular Velocity under Different Noise Levels

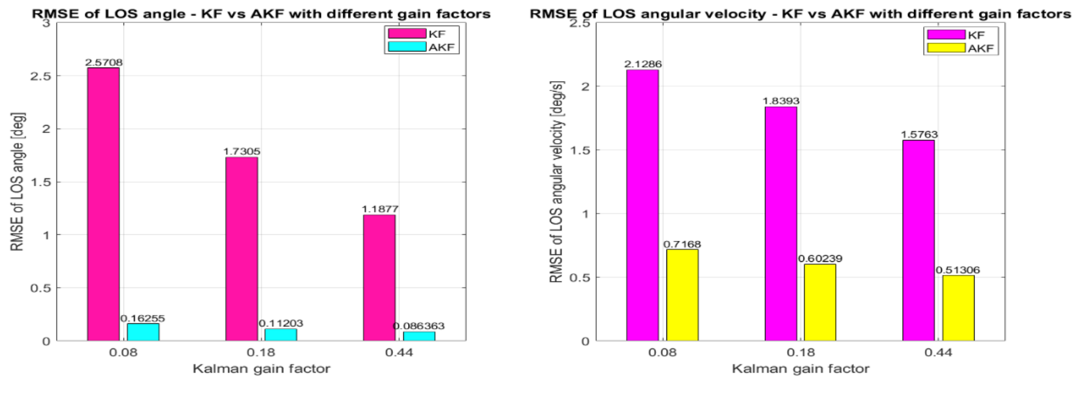

Figure 14. Comparison of Average RMSE of LOS Angle and Angular Velocity under Different Gain Factors

Figure 13 shows the change in RMSE for LOS angle and LOS angular velocity as the input noise level (σ) varies, and compares the performance of the standard KF and the AKF. It can be clearly seen that as the noise level increases from 0.03 to 0.36, the RMSE values of both quantities rise significantly, but the increase in KF is much higher than in AKF. Specifically, for the LOS angle, the RMSE of KF increases from

0.31419 (deg) to 2.6141 (deg) (more than eightfold), whereas AKF increases from only 0.017175 (deg) to 0.28257 (deg) (about sixteenfold, but the absolute value remains much smaller). Similarly, for LOS angular velocity, the RMSE of KF increases from 0.9649 (deg/s) to 2.1335 (deg/s), while AKF increases slightly from 0.22515 (deg/s) to 0.95074 (deg/s).

Figure 14 presents the change in RMSE for LOS angle and LOS angular velocity when varying the filter gain factor, in order to evaluate its influence on estimation performance in both KF and AKF. In general, as the gain increases from 0.08 to 0.44, the RMSE of both filters tends to decrease, indicating that a properly chosen gain improves convergence and reduces estimation error. However, the difference between the two filters is evident in terms of error reduction and stability. Specifically, for LOS angle, the RMSE of KF decreases from 2.5708 (deg) to 1.1877 (deg), while that of AKF varies only slightly from 0.16255 (deg) to 0.08636 (deg). For LOS angular velocity, KF decreases from 2.1286 (deg/s) to 1.5763 (deg/s), whereas AKF decreases more strongly from 0.7168 (deg/s) to 0.51306 (deg/s). This shows that AKF not only achieves lower RMSE but also maintains higher stability when the gain parameter changes.

3.5. Comparative Analysis between KF and AKF

The reason for this difference lies in the fact that KF uses a fixed gain coefficient based on the assumption of constant measurement and process noise, while AKF has a mechanism for adaptively adjusting the gain coefficient according to the variations of estimation errors and actual noise characteristics. Therefore, AKF responds more flexibly to changes in the measurement environment and target dynamics, achieving higher estimation accuracy and avoiding large error oscillations as in KF. These results demonstrate that using an adaptive gain allows the AKF to significantly reduce RMSE while ensuring greater stability and reliability in estimating LOS angle and angular velocity. This is a key advantage when applied to tracking systems for randomly maneuvering targets, especially under complex and time-varying noise conditions.

The results obtained from the simulations indicate that the adaptive mechanism reduces the RMSE by 4 to 6 times compared to the conventional KF under severe noise conditions. This significant improvement in tracking accuracy aligns with recent literature emphasizing adaptive and enhanced filtering techniques. Specifically, the robustness against noise uncertainty observed in the AKF corroborates the findings of (Ge et al., 2019; Kruse et al., 2025), who highlighted the necessity of noise compensation in time-varying environments. Furthermore, while neural-network-aided or high-order filters as proposed by (Stubberud & Kramer, 2023; Wu et al., 2025) offer complex architectural accuracy, our results demonstrate that a purely statistical-based adaptive noise variance update (as seen in Equations 18 and 20) remains a highly effective and computationally lightweight solution for fourth-order dynamics, directly addressing the phase lag commonly observed in fixed-gain designs.

4. Conclusion

Quantitative evaluation utilizing RMSE metrics confirms that the conventional KF is highly sensitive to noise variations, leading to increased estimation errors and phase lags during intense maneuvering phases. In contrast, the AKF maintains highly accurate and stable tracking performance by adaptively updating the noise covariance matrices in real time. This self-adjusting mechanism reduces the average error by up to 4-6 times, demonstrating the superiority and reliability of the adaptive filter for practical target-tracking applications.

However, this study has certain limitations. The current simulation model is restricted to a 2D planar motion and relies on partial linearization of target dynamics, which may not fully encapsulate complex 3D flight environments. Therefore, future work will focus on extending this adaptive mechanism to more robust nonlinear filtering frameworks, such as the Extended Kalman Filter (EKF) or the Unscented Kalman Filter (UKF), alongside validating the algorithm using real-world flight trajectory datasets to further verify its practical applicability.

References

Alanis, A. Y. (2025). Exploring Kalman Filtering Applications for Enhancing Artificial Neural Network Learning. *Algorithms*, *18*(9), 587. https://doi.org/10.3390/a18090587

Anagnostaki, I., Anastassopoulos, V., & Koukiou, G. (2026). Applications of the Kalman Filter in Physical Processes: A Review. *Applied Sciences*, *16*(10), 4649. https://doi.org/10.3390/app16104649

Chen, X., Lin, D., Li, H., & Cheng, Z. (2025). Minimum error entropy high-order extend Kalman filter with fiducial points. *Applied Mathematics and Computation*, *487*, 129113. https://doi.org/10.1016/j.amc.2024.129113

Ding, L., & Wen, C. (2024). High-Order Extended Kalman Filter for State Estimation of Nonlinear Systems. *Symmetry*, *16*(5), 617. https://doi.org/10.3390/sym16050617

Eang, C., & Lee, S. (2024). An Integration of Deep Neural Network-Based Extended Kalman Filter (DNN-EKF) Method in Ultra-Wideband (UWB) Localization for Distance Loss Optimization. *Sensors*, *24*(23), 7643. https://doi.org/10.3390/s24237643

Ge, B., Zhang, H., Jiang, L., Li, Z., & Butt, M. M. (2019). Adaptive Unscented Kalman Filter for Target Tracking with Unknown Time-Varying Noise Covariance. *Sensors*, *19*(6), 1371. https://doi.org/10.3390/s19061371

Habib, M., Elomari, Y., Hochwallner, F., Buruzs, A., Barz, T., & Wang, Q. (2025). Extended Kalman filter on sparse identification of nonlinear systems: application to the SoC estimation of a phase change material-based energy storage. *Energy Conversion and Management: X*, *27*, 101199. https://doi.org/10.1016/j.ecmx.2025.101199

Kruse, T., Griebel, T., & Graichen, K. (2025). Adaptive Kalman Filtering: Measurement and Process Noise Covariance Estimation Using Kalman Smoothing. *IEEE Access*, *13*, 11863–11875. https://doi.org/10.1109/ACCESS.2025.3528348

Mursyitah, D., Faizal, A., & Sari, S. P. (2025). Algorithm Design and Programming the Luenberger Observer for level estimation in a Storage Tank System. *Indonesian Journal of Informatic Research and Software Engineering (IJIRSE)*, *5*(1), 79–87. https://doi.org/10.57152/ijirse.v5i1.2065

Peng, D., Wen, C., & Lv, M. (2023). Design of a High-Order Kalman Filter for State and Measurement of A Class of Nonlinear Systems Based on Kronecker Product Augmented Dimension. *Sensors*, *23*(6), 2894. https://doi.org/10.3390/s23062894

Sheikh, C. S. M. (2023). System State Estimation Using Weighted Least Square Method. *Proceeding International Conference on Science and Engineering*, *11*(1), 1294–1299. https://doi.org/10.52783/cienceng.v11i1.276

Stubberud, S. C., & Kramer, K. A. (2023). *Neural Extended Kalman Filter Tracker Using the ReLu Function* (pp. 236–241). https://doi.org/10.1007/978-3-031-40579-2_23

Wang, R., & Shen, Z. (2024). A Deep Neural Network-Ensemble Adjustment Kalman Filter and Its Application on Strongly Coupled Data Assimilation. *Journal of Marine Science and Engineering*, *12*(1), 108. https://doi.org/10.3390/jmse12010108

Wu, W., Liu, J., Zhang, J., Guo, J., Hu, J., Zhang, F., & Wang, C. (2025). Deterministic learning based extended kalman filter for nonlinear dynamics modeling. *Journal of the Franklin Institute*, *362*(18), 108175. https://doi.org/10.1016/j.jfranklin.2025.108175